Desalting plasma protein solutions by membrane capacitive deionization

Bharat Shrimant[a], Tanmay Kulkarni[a], Mahmudul Hasan[a], Charles M. Arnold[b], Nazimuddin Khan[b], Abhishek N. Mondal[c], Christopher G. Arges[a*]

[a]Department of Chemical Engineering, Pennsylvania State University, University Park, PA 16802, USA

[b]CSL Behring, Bradley, IL 60915, USA

[c]Donaldson Company Inc., Bloomington, MN 55431, USA

[*]Corresponding author: email: chris.arges@psu.edu

Abstract

Plasma protein therapies are used by millions of people across the globe to treat a litany of diseases and serious medical conditions. One challenge in the manufacture of plasma protein therapies is the removal of salt ions (e.g., sodium, phosphate, and chloride) from the protein solution. The conventional approach to remove salt ions is the use of diafiltration membranes (e.g., tangential flow filtration) and ion-exchange chromatography. However, the ion-exchange resins within the chromatographic column, as well as filtration membranes, are subject to fouling by the plasma protein. In this work, we investigate membrane capacitive deionization (MCDI) as an alternative separation platform for removing ions from plasma protein solutions with negligible protein loss. MCDI has been previously deployed for brackish water desalination, nutrient recovery, mineral recovery, and removing pollutants from water. However, this is the first time this technique has been applied for removing 28% of ions (sodium, chloride, and phosphate) from human serum albumin solutions with less than 3% protein loss from the process stream. Furthermore, the MCDI experiments utilized highly conductive poly(phenylene alkylene) based ion exchange membranes (IEMs). These IEMs combined with ionomer coated nylon meshes in the spacer channel ameliorate ohmic resistances in MCDI improving energy efficiency. Overall, we envision MCDI as an effective separation platform in biopharmaceutical manufacturing for deionizing plasma protein solutions and other pharmaceutical formulations without loss of active pharmaceutical ingredients.

Keywords Membrane capacitive deionization, poly(phenylene alkylene) ion exchange membranes, plasma proteins, albumin

Introduction

Proteins are important macromolecules to all forms of life as they influence cell metabolism, the immune system of living organisms, and perform other important bodily activities.[1] Human serum albumin (HSA) is the most abundant protein in the human body and has many applications in medical fields such as replacing lost albumin in patients with hypoalbuminemia, treating hypovolemia, as a part of some diagnostic imaging kits, and as a supplement for cell culture.[2] [3] [4] HSA is one type of plasma-derived protein used for numerous therapies. In addition to HSA, there are other plasma proteins, such as globulins/ immunoglobulins and fibrinogen, that are also used as therapies to treat a variety of diseases and medical conditions.[5] [6] [7]

The processing of plasma protein formulations for medical use entails multiple separation units such as chromatography, filtration, and dialysis.[8] [9] [10] [11] [12] One notable challenge in the separation process is the removal of inorganic salt ions from the plasma protein process stream without diluting or losing the plasma protein from the process stream. Ion exchange column chromatography using resin particles, dialysis, gel filtration and ultra/di-filtration membranes are often deployed to remove excess salt, such as sodium chloride and phosphate salts from the process stream containing the plasma protein.[13] [14] [15] However, these approaches are either time consuming, increase sample volumes, or the membranes and resins used are prone to fouling by the proteins.[16] [17] [18] Protein fouling in particular is catastrophic as it is the most valuable material in the stream and any loss increases manufacturing costs. It is also worth mentioning that ion-exchange chromatography necessitates chemicals for regenerating the resin bed and this leads to process waste and a longer separation process. Devising a separation unit that can directly deionize the protein solution without concern of protein fouling while also having short down times will benefit plasma protein manufacturing operations.

Electrodialysis (ED), electrodeionization (EDI), and capacitive deionization (CDI)/membrane capacitive deionization (MCDI) are commercial electrochemical separation processes used for removing ions from solutions.[19] In addition to being deployed for desalination, they have also been used for heavy metal ion removal, organic acid removal, nutrient recovery, and recovery of critical minerals.[20] [21] [22] [23] [24] In the context of deionizing plasma protein solutions, EDI is ill-suited because the unit features ion-exchange resins that are prone to fouling. ED, the most mature electrochemical deionization process, suffers from severe ohmic losses in the process stream when

a good portion of the ions are removed. In practice, ED will have its polarity flipped, known as electrodialysis reversal (EDR), to prevent ion-exchange membrane fouling by surfactants – which are charged macromolecules that have some resemblance to proteins. CDI and MCDI are less mature electrochemical deionization platforms. They have attracted notable attention in recent years for deionizing brackish water streams because energy can be recovered during the electrode regeneration step resulting in a low specific energy consumption for desalination.[25] Like EDR, CDI and MCDI flip the cell polarity to regenerate the electrodes. This polarity reversal would make CDI and MCDI less amenable to fouling by charged macromolecules, such as proteins. MCDI differs from CDI because it has ion-exchange membranes (IEMs) that cover the porous electrodes to prevent co-ion adsorption and to promote current utilization during deionization.[26]

In the CDI and MCDI processes, a cell voltage difference is applied to two porous electrodes. An anion exchange membrane (AEM) covers the positively biased electrode in MCDI to remove anions from the process stream while a cation exchange membrane (CEM) covers the negatively biased electrode to remove cations. The removed ions are stored in the electrochemical double layer of the porous, activated carbon electrodes.[27] After a period of deionization, the direction of the electrical current for the cell is reversed to regenerate the porous electrodes. This discharge steps leads to ion removal from the electrodes (i.e., regeneration) and a more concentrated salt solution.[28] Notably, MCDI, like other electrochemical deionization platforms, operates under mild, ambient conditions whereas distillation and membrane filtration, which are the conventional separation platforms used in chemical processes, necessitate high pressure and elevated temperatures. These extreme conditions can damage the protein in solution.

In this work, we investigated MCDI for deionizing HSA solutions containing dissolved sodium chloride and monosodium dihydrogen phosphate (NaH_2PO_4). Prior to performing deionization experiments with HSA, we examined MCDI performance at different NaCl and/or NaH_2PO_4 feed concentrations with highly conductive poly(phenylene alkylene) IEMs and porous meshes coated with poly(phenylene alkylene) ionomers. Our previous work showed that IEMs' with $\geq$ 4x reduction in area specific resistance (ASR) resulted in a 2x increase in the energy normalized adsorbed salt (ENAS – inversely commensurate to specific energy consumption). Hence, IEMs that are more conductive and thinner improve the energy metrics of MCDI.[29] In a subsequent report, we used ionomer coated nylon meshes placed in the spacer channel (where the process

stream passes through) to augment the process stream ionic conductivity.[30] This resulted in ≥ 2x increase in the ENAS values when compared to a MCDI process that did not have a porous ionic conductor. The ionomer materials deployed in our previous work used poly(arylene ether) backbones. These materials have lower ionic conductivity when compared to the more recent poly(phenylene alkylene) ionomers developed for fuel cell and electrolysis applications.[31] [32] [33] Here, we show that the highly conductive poly(phenylene alkylene) ionomers used as IEMs and porous ionic conductors are effective for deionizing NaCl and NaH_2PO_4 salt solutions (single salt in water or a mixture of salts in water) at different concentrations (up to 8 g L^{-1}). Additionally, we also show that the said ionomer materials implemented in MCDI are effective for deionizing salt-plasma protein mixtures with 18 to 28% salt removal while demonstrating negligible loss (< 3%) of albumin from the process stream. Overall, MCDI with advanced ionomer materials is an effective deionization platform for plasma protein solutions.

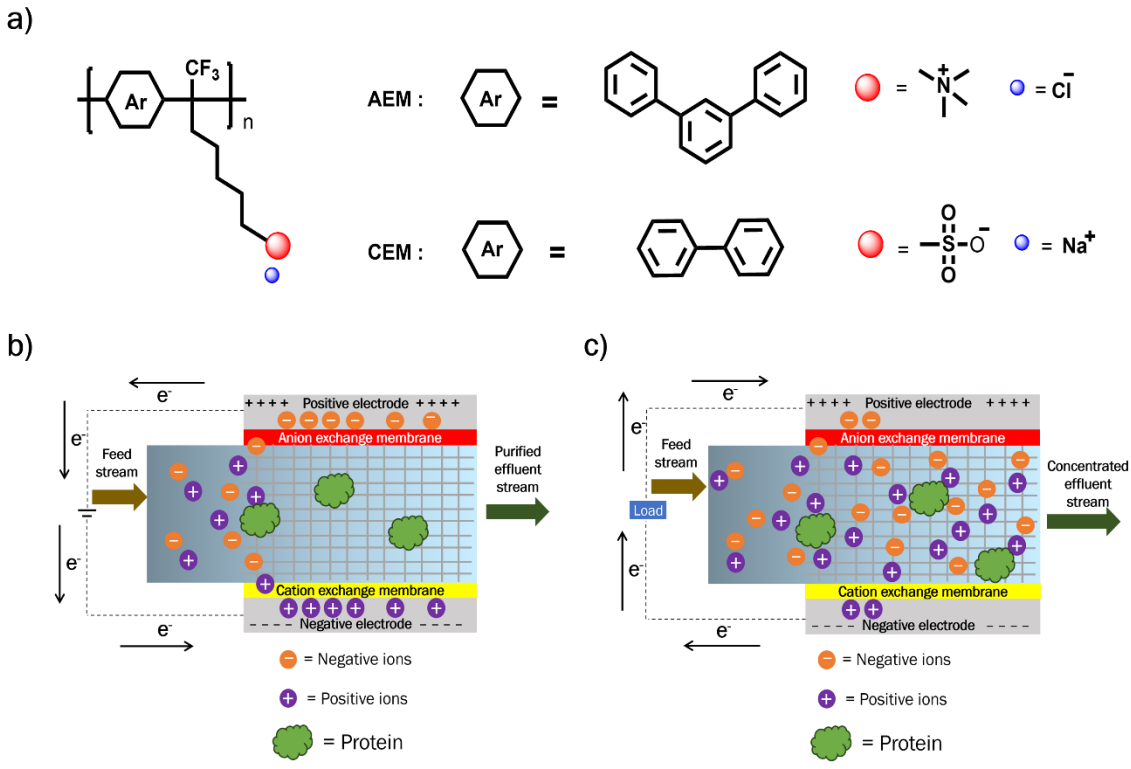

Figure 1. (a) Structures of ion exchange membranes. MCDI process flow schemes for (b) charge/deionization cycle and (c) discharge/regeneration cycle.

Results and Discussion

Synthesis and properties of IEMs

IEMs for MCDI should display high ionic conductivity while also demonstrating low water uptake (WU) and strong mechanical properties.[34] High water uptake leads to excessive swelling of membranes within the cell jeopardizing mechanical properties. The poly(phenylene alkylene) IEMs in this work have excellent ionic conductivity because of their high IEC values (2.1 to 2.4 mequiv g^{-1}, (**Table 1**). Furthermore, the all-carbon, aromatic repeat units of m-terphenyl and biphenyl in these ionomers suppress water uptake and swelling ($\leq$ 26 % WU and $\leq$ 9% SR (**Table 1**). [31, 35] The chemical structures of the poly(phenylene alkylene) AEMs and CEMs are shown in **Figure 1**. There has only been one report investing the class of poly(phenylene alkylene) ionomers for MCDI.[36] This recent article investigated poly(fluorene) backbone anion exchange ionomer and cation exchange ionomer variants and compared the electrode salt capacity and charge efficiency of CDI, MCDI with commercial ASTOM IEMs, and MCDI where the poly(fluorene) ionomers coated the porous electrodes. The article only examined deionization of a single concentration of 500 ppm NaCl in water.

The poly(phenylene alkylene) IEMs used in this work were prepared by superacid-catalyzed polymerization of aromatics (m-terphenyl and biphenyl) and 7-bromo-1,1,1-trifluorohexane-2-one as depicted in **Schemes S1** and **S2**. The trimethylammonium group was introduced into the AEM by the Menshutkin reaction of the alkylated bromide functionality in m-TPBr with trimethylamine. The cation exchange membrane was prepared by two different synthetic routes. In the first route, biphenyl backbone with alkylated bromide functionality (BPBr) was reacted with potassium thioacetate followed by oxidation of thioacetate group to sulfonic acid group using hydrogen peroxide in formic acid. After the heterogeneous oxidation reaction, the CEM was not soluble in any solvent. In the second synthetic route approach, the thioacetate group was oxidized to sulfonic acid group using *m*-chloroperbenzoic acid (m-CPBA) to obtain soluble cation exchange ionomer. The ^{1}H NMR spectra substantiating the polymer structures are provided in **Figures S1-S5**. The Mn values of the poly(phenylene alkylene) precursors with terminal bromo groups ranged from 45 to 78 kDa. These values were determined by GPC.

Most MCDI studies deploy commercially available IEMs used in electrodialysis. For benchmarking purposes, we compared the ionic conductivity, water uptake, and swelling ratio of the poly(phenylene alkylene) IEMs against commercially available IEMs from Fumatech. The poly(phenylene alkylene) IEMs showed 3x higher ionic conductivity (or more) than the Fumasep

IEMs (**Table 1**). Because the poly(phenylene alkylene) IEMs are almost 2x thinner than the Fumatech IEMs, their ASR values are at least 6x lower. The poly(phenylene alkylene) IEMs' water uptake (**Table 1**) is slightly higher than the Fumasep IEMs (20 to 26% versus 15 to 17%), but the swelling ratios between the two classes of the IEMs are about the same. The poly(phenylene alkylene) backbones were effective for suppressing water uptake. The high ionic conductivity and low swelling ratio of the poly(phenylene alkylene) IEMs make them good candidates for MCDI.

Table 1. Ion-exchange membrane (IEM) properties

Membrane type	**Thickness (μm)**	**IEC (mequiv g^{-1})**	**WU (%)**	**SR (%)**	**κ (mS/cm) in DI water**	**ASR (ohm cm^2)**
Fumasep CEM	75	1.5	17	7	10.0	0.8
Fumasep AEM	75	1.3	15	4	4.4	1.7
BPSA CEM	30	2.4	26	9	29.8	0.1
m-TPN1 AEM	41	2.1	20	5	14.7	0.3

MCDI experiments without HSA

Prior to deionizing plasma protein solutions, initial experiments were performed to test how effective poly(phenylene alkylene) IEMs and porous ionic conductors for deionizing NaCl and NaH_2PO_4 feed solutions. The first set of experiments compared MCDI performance with a 250 ppm NaCl feed using poly(phenylene alkylene) IEMs and Fumatech IEMs. Then, MCDI experiments were performed with poly(phenylene alkylene) IEMs with a porous ionic conductor in the spacer channel and no porous ionic conductor in the spacer channel with 250 ppm $NaCl_{aq}$ feeds. These experiments were performed with low NaCl feed concentrations to accentuate how the ASR values of the IEMs and porous ionic conductors affect MCDI energy use.

After establishing that poly(phenylene alkylene) IEMs and porous ionic conductors were more effective than Fumatech IEMs and MCDI with no porous ionic conductors, a series of MCDI experiments were performed with 8000 ppm NaCl and 6000 ppm NaH_2PO_4. These experiments used poly(phenylene alkylene) IEMs and examined the scenarios with a porous ionic conductor

and no porous ionic conductor. It is important to note that most MCDI studies examine model brackish water feeds (≤ 5000 ppm NaCl). However, the salt concentration in plasma protein solutions is often higher than brackish water streams.

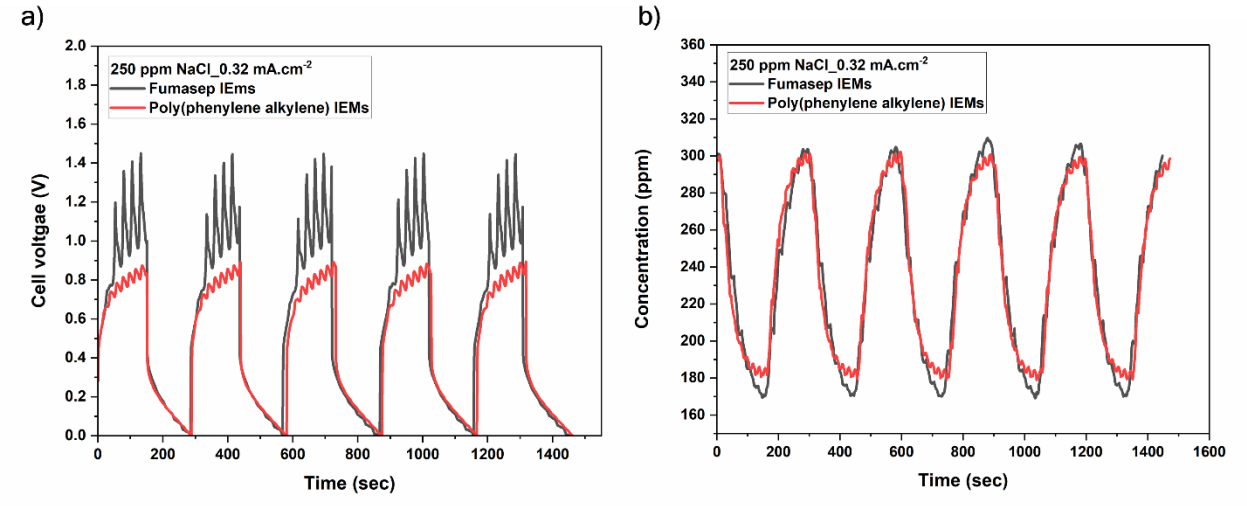

Figure 2. (a) Cell voltage versus time and (b) effluent NaCl concentration versus time for charge-discharge cycling at a constant current density of ± 0.32 mA cm^{-2} in MCDI for 250 ppm NaCl feed with Fumasep IEMs (black) and poly (phenylene alkylene) IEMs (red).

Figures 2a and **2b** show charge-discharge cell voltage and effluent concentration curves for 250 ppm NaCl feed for MCDI featuring poly(phenylene alkylene) IEMs and Fumatech IEMs. **Table S1** provides the salt removal efficiency (SRE), columbic efficiency (CE), and average salt absorption rate (ASARj) from the MCDI experiments with this salt feed concentration and at a constant current density (0.32 mA cm^{-2}). Because the MCDI unit was operated under constant current, the SRE, CE, and ASAR were relatively the same between experiments with the different types of IEMs. However, there was a significant difference in the cell voltage curves between the two configurations. The adoption of the more conductive poly(phenylene alkylene) IEMs reduced the cell voltage by 300 mV during the charge step. During the MCDI experiments, EIS was performed to assess differences in the high frequency resistance (HFR). From the HFR values shown in the Nyquist plot (**Figure S8**), the cell HFR was reduced by 24% when using the poly(phenylene alkylene) IEMs as opposed to the Fumatech IEMs. The HFR values (aka R_s) are provided in **Table S3**. The energy recovery values, as well as the energy use upon charging and

discharging, with the MCDI unit with a 250 ppm feed for the two different sets of IEMs are provided in **Table S1**. From the control case of MCDI with no porous ionic conductor and using electrodialysis IEMs (Fumasep), the ENAS was 21% higher when using poly(phenylene alkylene) IEMs and no porous ionic conductor. The ENAS value is inversely commensurate to the HFR (i.e., a reduction in HFR yields a larger ENAS value).

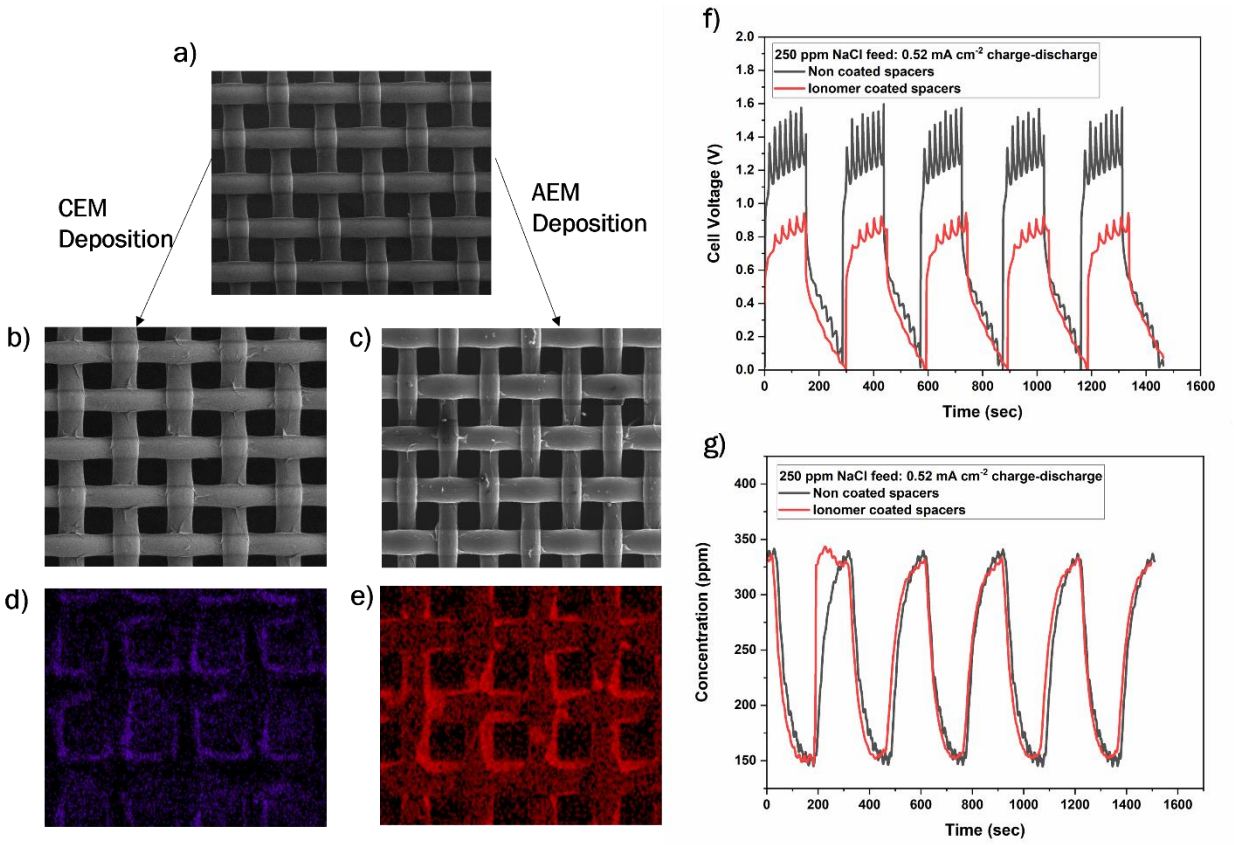

Figure 3. SEM images of (a) pristine nylon mesh (b) CEM coated nylon mesh and (c) AEM coated nylon mesh. EDX maps of (d) CEM coated nylon mesh and (e) AEM coated nylon mesh. (f) Cell voltage versus time and (g) effluent NaCl concentration profile for charge-discharge cycles in MCDI for 250 ppm NaCl with non-coated (black) and ionomer coated (red) nylon meshes in the spacer channel.

The next set of experiments compared MCDI performance with porous ionic conductors in the spacer compartment and no porous ionic conductor in the spacer compartment with poly(phenylene alkylene) IEMs. As the process stream becomes deionized, the ohmic resistance in the spacer compartment becomes substantial and hinders the energy efficiency of the MCDI process. We coated poly(phenylene) anion exchange ionomer on one sheet of nylon mesh via aerosol spray deposition to a loading of 2.4 mg cm^{-2}. Then, poly(phenylene) cation exchange

ionomer on an identical bare nylon sheet was deposited until a loading of 2.4 mg cm^{-2} was attained. **Figure 3a-e** present electron micrographs of the porous nylon mesh with and without ionomer coatings. This Figure also gives EDX images substantiating the presence of the sodium and bromide counterions in the ionomer coated nylon meshes before running MCDI experiments. **Figure 3f** and **3g** shows the MCDI charge-discharge cell voltage and effluent concentration curves for a 250 ppm NaCl with non-coated and ionomer coated meshes in the spacer channel. Nylon meshes coated with the highly conductive poly(phenylene alkylene) ionomers reduced the cell voltage by 500 mV when operating at a constant current of 0.52 mA cm^{-2}. A higher current density was used in the deionization and electrode regeneration step in these experiments because the poly(phenylene alkylene) IEMs reduced the cell's ohmic resistance. The SR and ASAR values, reported in **Table S2**, were identical for both configurations (ionomer coated nylon meshes and non-coated nylon meshes) because both experiments were operated at the same current density. **Table S2** also provides the energy use and recovery values for these two configurations. **Figure S9** provides the Nyquist plot attained from EIS during MCDI experiments. The porous ionic conductors reduced the HFR by 22 %. The ENAS values for MCDI with 250 ppm NaCl feed and operating at 0.52 mA cm^{-2} increased by 40% when using a porous ionic conductor. The ENAS values for the MCDI experiments with and without porous ionic conductors and poly(phenylene alkylene) IEMs with 250 ppm NaCl feeds are given in **Table S2**.

After establishing the effectiveness of poly(phenylene alkylene) ionomer materials for MCDI, the next set of experiments investigated deionization of higher salt feed concentrations such as 8000 ppm NaCl and 6000 ppm NaH_2PO_4 solutions. At the onset of the experiments, it was unclear if the porous ionic conductors would still be effective for augmenting spacer channel conductivity given the higher feed concentration and performing a single-pass MCDI assessment. **Figures 4a-4d** present the MCDI voltage versus time and effluent concentration versus time for 8000 ppm NaCl feeds and 6000 ppm NaH_2PO_4 feeds. The MCDI operating parameters with the said feed solutions are provided in **Table S2**. The salt removal efficiency decreased from the mid-50% to 28 to 33% when increasing feed concentration from 250 ppm NaCl to 8000 ppm NaCl and 6000 ppm NaH_2PO_4. The drop in the SRE arises from the larger amount of salt in the feed while keeping the cell active area constant. A bigger cell area would provide a large SRE. When operating MCDI at 6 mA cm^{-2} for the 8000 ppm NaCl feed with or without a porous ionic conductor, it is worth noting that the change in effluent concentration was 2500-3000 ppm for 25 cm^2 active area. Although an

8000 ppm NaCl feed solution is sent through the MCDI, the traces in **Figure 4b** show an apex value of 10,000 ppm NaCl. This occurs because the first 3 charge-discharge cycles are excluded as part of a cell conditioning protocol in our lab. During the electrode regeneration/discharge cycle step, the salt adsorbed in the porous electrode is removed and added to the 8000 ppm NaCl feed leading to a brine solution of about 10,000 ppm.

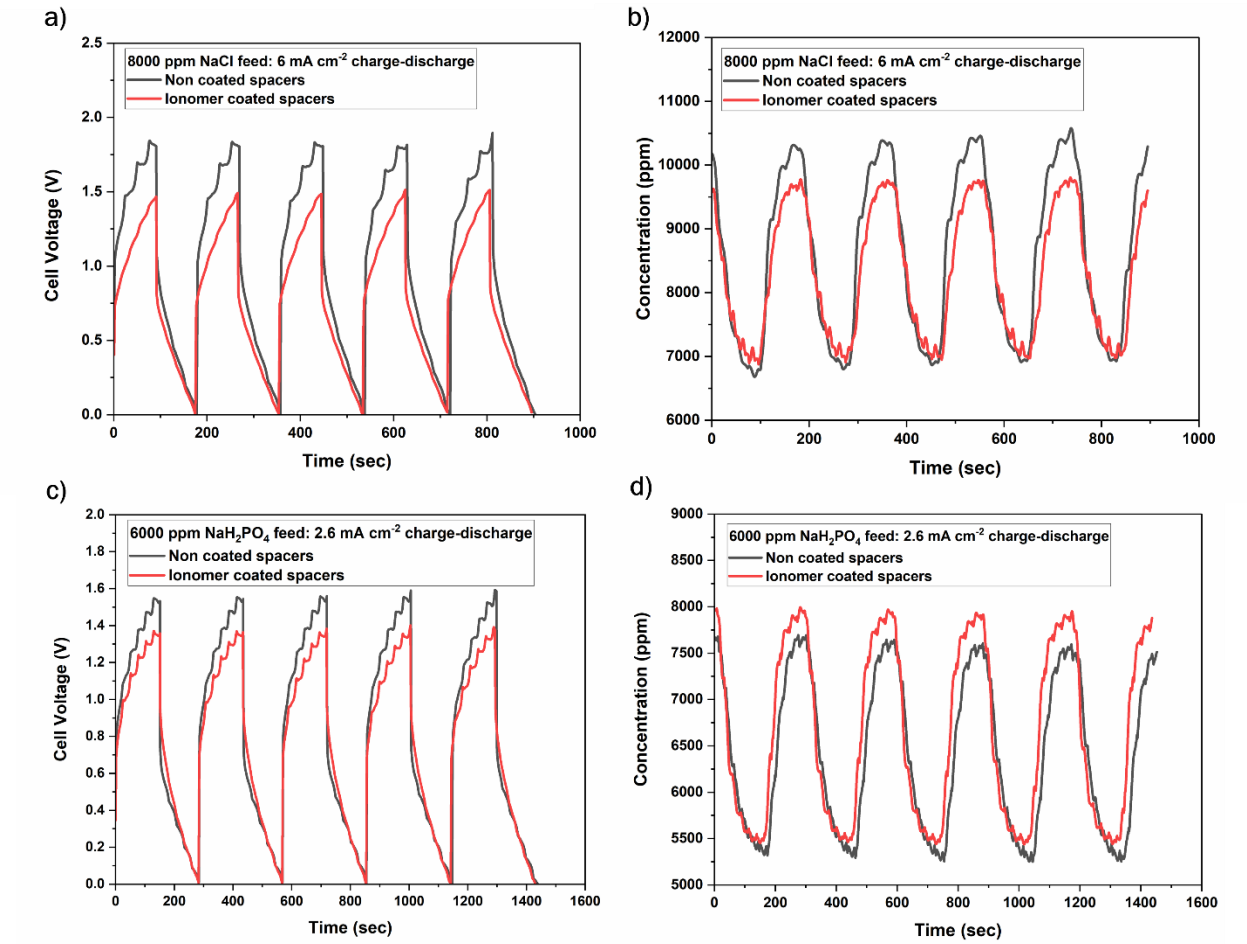

Figure 4. (a) Cell voltage versus time and (b) effluent NaCl concentration versus time for charge-discharge cycles in MCDI for 8000 ppm NaCl with non-coated (black) and ionomer coated (red). (c) Cell voltage versus time and (d) effluent NaH_2PO_4 concentration versus time for charge-discharge cycles in MCDI for 6000 ppm NaH_2PO_4 with non-coated (black) and ionomer coated (red).

It is worth noting that most MCDI papers examining new electrode or IEM materials use synthetic brackish water streams mostly composed of NaCl $\leq$ 5000 ppm in deionized water. However, the

plasma protein solutions contain a lot more NaCl, and hence we demonstrated that the poly(phenylene alkylene) IEMs are effective for deionizing higher concentration salt feeds in MCDI. We anticipate that a greater salt removal efficiency is possible by using a larger active area with additional cells in series. Another pathway for more salt removal involves using two liquid streams: 1) a recirculating plasma protein stream that is being deionized and 2) a waste brine stream that is used for electrode regeneration. This latter approach will be discussed in further detail later. Finally, we also wish to point out that the nylon meshes coated with poly(phenylene alkylene) ionomer were effective for augmenting spacer channel ionic conductivity with NaCl concentrations of 6000 to 10,000 ppm resulting in about a 300 mV lower cell voltage when running the unit at 6 mA cm^{-2}.

Plasma protein formulations often contain phosphate salts as a buffering agent. There have been few reports on using MCDI to remove phosphate anions from aqueous streams – mostly in the context of phosphorus recovery from fertilizer runoff.[37] [38] Our first experiments attempting to deionize NaH_2PO_4 aqueous solutions led to poor SRE values at various cell voltages (as high as 2 V). This observation is in-line with another literature report using a high cell voltage to deionize phosphate solutions.[39] The problem was remediated by letting a 250 ppm NaH_2PO_4 solution sit in the spacer compartment of an assembled MCDI cell with poly(phenylene alkylene) IEMs with and without a porous ionic conductor for 12 to 16 hours before running deionization experiments. This conditioning step allowed us to attain SR values of 28% and below a cell voltage of 1.5 V when using a 6000 ppm NaH_2PO_4 feed and operating the MCDI at 2.6 mA cm^{-2}. **Figures 4c** and **4d** present the cell voltage versus time and the NaH_2PO_4 effluent concentration versus time during charge-discharge cycling in the cell. Similar to the 8000 ppm NaCl MCDI experiments, it is important to note that the discharge cycle during MCDI leads to a peak effluent concentration of 7600 to 8000 ppm NaH_2PO_4. Finally, a porous ionic conductor in the MCDI setup reduced the cell voltage by 200 mV when deionizing 6000 ppm NaH_2PO_4 at 2.6 mA cm^{-2}. The lower cell voltage drop when using a porous ionic conductor for 6000 ppm NaH_2PO_4 compared to using a porous ionic conductor with NaCl feeds was attributed to the lower ionic mobility of the dihydrogen phosphate anion over the chloride anion. **Figure S11** gives the Nyquist plot for deionizing 6000 ppm NaH_2PO_4 at 2.6 mA cm^{-2} with and without porous ionic conductors. The HFR value decreased by 5% when ionomer coated spacers were used. **Table S2** reports the SRE, energy recovery, and ENAS values for deionizing 6000 ppm NaH_2PO_4 feed solutions. Overall, **Figure 4** demonstrates

that poly(phenylene alkylene) ionomer materials, used as IEMs and coatings on nylon meshes in the spacer channel, is effective for deionizing process streams with over > 5 g L^{-1} salt solutions.

MCDI experiments with HSA-salt solutions

The final set experiments tested the extent of plasma protein solution deionization while co-currently assessing if any HSA was lost during the deionization process. **Figures 5a-5f** report the effluent stream conductivity during charge-discharge cycling in MCDI with a feed stream of 5800 ppm NaCl mixed, 2400 ppm sodium phosphate, and 5, 10 or 20 mg mL^{-1} of HSA. We test this HSA concentration range as it corresponds to a model process stream in biopharmaceutical manufacturing. Plus, we also wanted to assess if higher concentrations of HSA would exacerbate fouling.

Figures 5b, 5d and **5f** show a 18-20% drop in effluent stream ionic conductivity while showing 1 to 3% HSA loss – a negligible and acceptable loss. In previous MCDI experiments with a single salt in the feed stream, an ionic conductivity calibration curve could be used to determine effluent stream concentration. However, ionic conductivity cannot discriminate between the different concentrations in ions. Inductively coupled plasma-optical emission spectrometry (ICP-OES) was used to quantify the amount of sodium and phosphate removed from the process stream. The difference between the amount of phosphate removed and sodium removed was equivalent to the amount of chloride removed. **Tables S5-S7** report the amount of sodium, phosphate, and chloride removed upon the charge-discharge cycles that correspond to **Figures 5a-5f**. UV-Vis was used to assay the HSA concentration in the effluent stream during various time points during the charge-discharge cycling. **Figure S12** provides the raw UV-Vis data for collected, and diluted, process stream solutions. Overall, there is negligible change in the absorption peak affiliated with HSA. Overall, **Figure 5** conveys successful salt removal from HSA solutions in a single-pass setup. Further deionization necessitates a large cell area, multiple cells, or recirculation of the process stream.

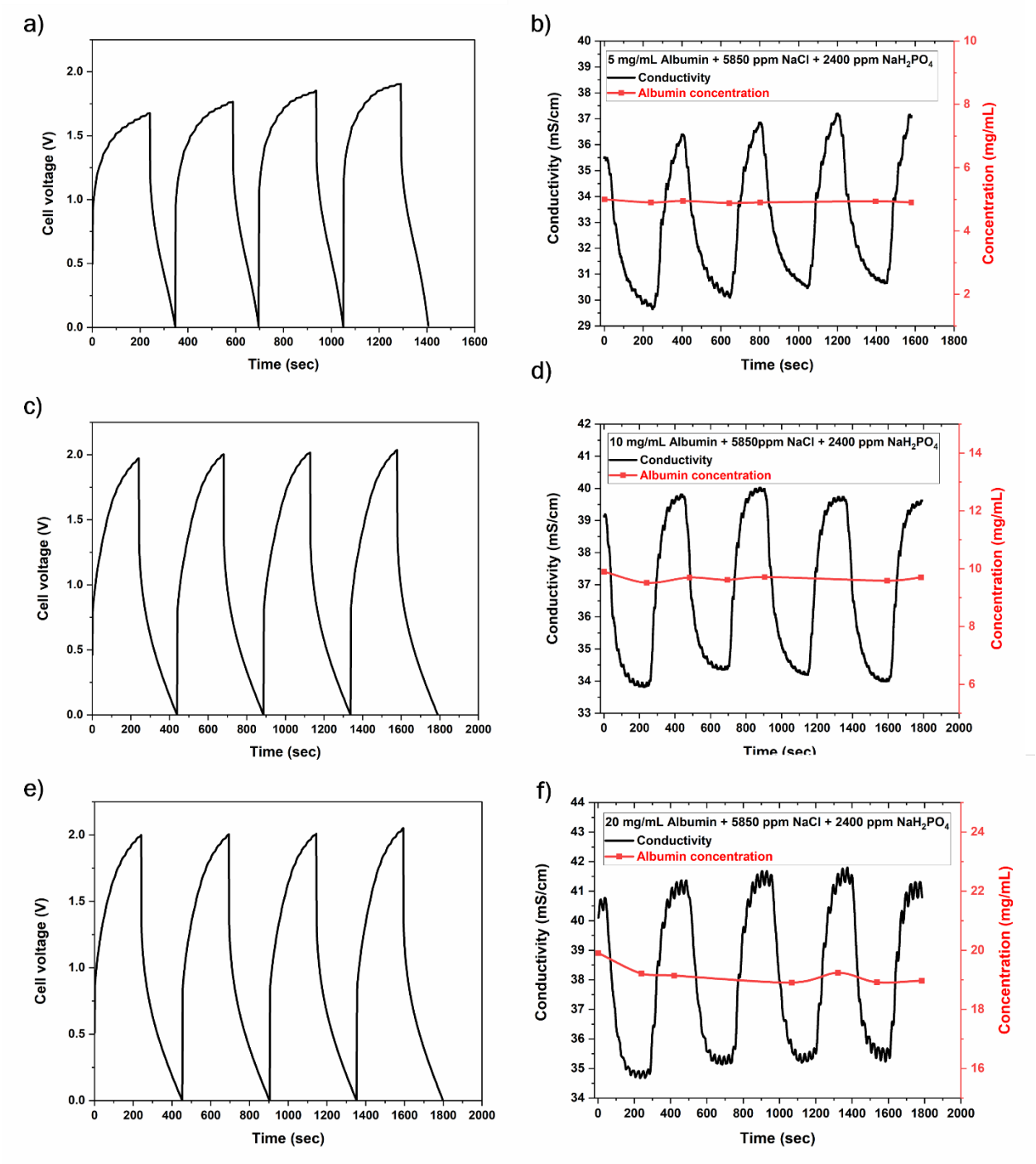

Figure 5. Cell voltage versus time and effluent conductivity versus time and albumin concentration vs time for charge-discharge cycling at a constant current density of ± 3 mA cm^{-2} in MCDI for the following albumin concentration in the fee: (a) and (b) 5 mg/mL HSA, (c) and (d) 10 mg/mL HSA and (e) and (f) 20 mg/mL HSA.

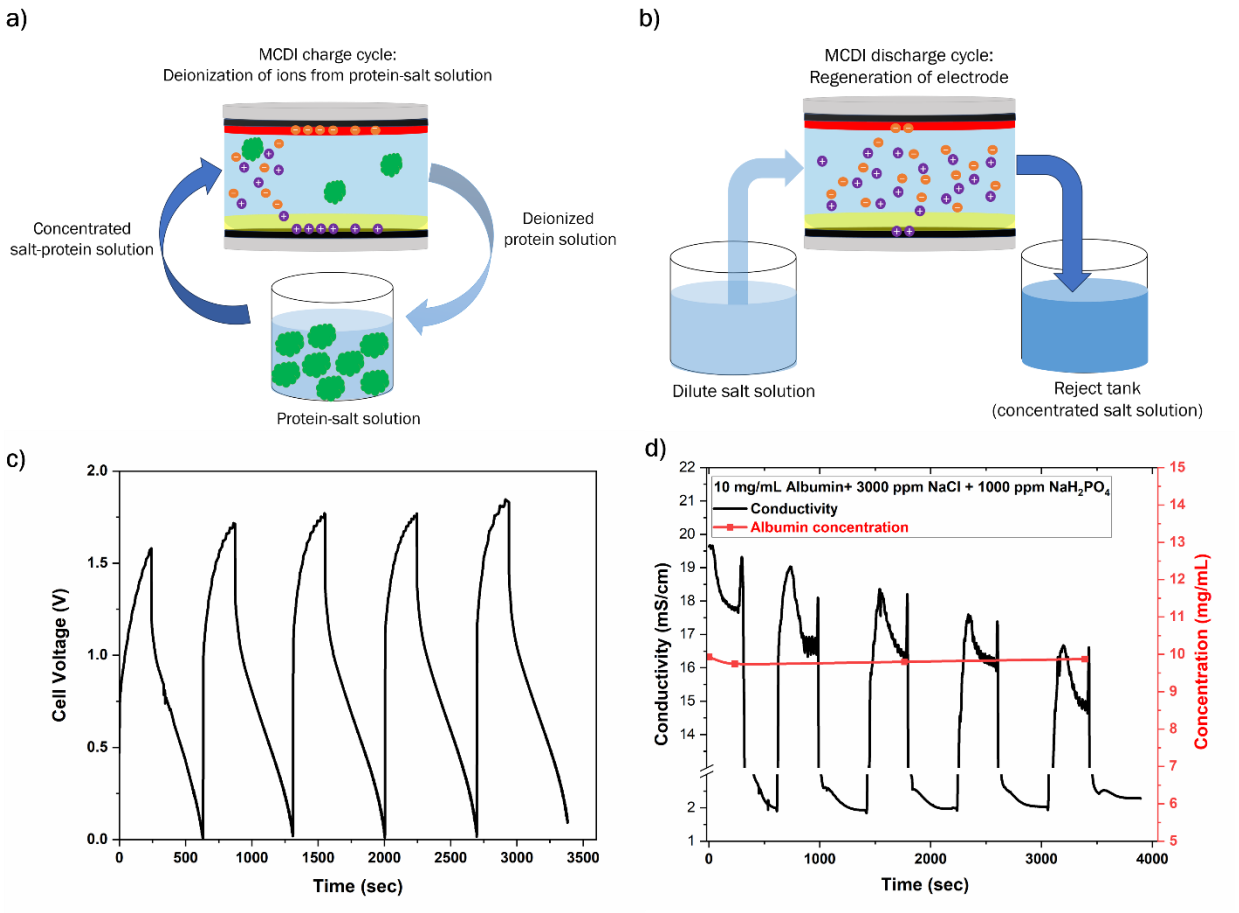

Figure 6. MCDI process flow schemes for recirculation method for (a) charge cycle/deionization and (b) discharge/regeneration cycle. (c) Cell voltage versus time and (d) effluent conductivity vs time and HSA concentration versus time. Charge cycle conditions: Feed: 10 mg/mL HSA + 3000 ppm NaCl + 1000 ppm NaH_2PO_4, current: 1.8 mA/cm2, time: 240 sec. Discharge cycle conditions: Feed: 250 ppm NaCl, current: 0.6 mA/cm2, time: set to 0 V.

The last set of experiments recirculated the plasma protein stream so a greater extent of deionization in the plasma protein solution can be achieved. **Figure 6a** conveys the recirculation strategy. For this experiment, the process stream consisted of 3000 ppm NaCl mixed with 1000 ppm NaH_2PO_4 and 10 mg mL^{-1} of HSA feed. The process stream only passed through the MCDI unit during charge/deionization step. This stream was recirculated through the unit during the charge/deionization step. During discharge mode to regenerate the electrodes, the feed solution to the MCDI was changed to a low concentration of NaCl (250 ppm) feed (**Figure 6b**). **Figures 6c** and **6d** present the cell voltage versus time and the effluent conductivity versus time during charge-discharge cycling and the HSA concentration in the effluent. The conductivity of the plasma

protein solution continued to decrease over multiple charge cycles (i.e., time). For instance, the initial conductivity of the first charge cycle was 19.5 mS/cm while the initial conductivity of fifth cycle was 16.3 mS/cm indicating ions are being removed from feed stream for every charge cycle. The ICP-OES data for chloride and phosphate concentration with different charge cycles are provided in **Table S8**. Using the recirculation strategy, 28% of the salt in the plasma protein solution was removal from the feed stream. During the recirculation, there was negligible loss of protein (**Figure 6d**). As the salt is removed from the plasma protein solution, the cell voltage slightly climbs with each cycle as the concentration of ions in the solution is reduced. This problem can be addressed by reducing the cell current density with each cycle. Overall, the recirculation method for deionizing plasma protein solutions, as well as other ion containing solutions, has many advantages as it can lead to deeper deionization extents and it does not need multistage separation. Future work will look to optimize this process and compare against the advantages of a large cell and multiple MCDI units in series (or hybrid units in series electrodialysis followed by MCDI).

Conclusions

In this study, poly (phenylene alkylene) based ion exchange membranes were tested in MCDI cells that allow for the deionization of relatively high (up to 8,000 ppm) sodium chloride and monosodium phosphate solutions in aqueous and protein solutions. Due to the high conductivity and low ASR values, poly(phenylene alkylene) IEMs MCDI configuration displayed better performance than the commercial Fumasep IEMs MCDI configuration. Ohmic resistance in the spacer channel of the MCDI was ameliorated by incorporating poly (phenylene alkylene) ionomer-coated nylon meshes. The use of these porous ionic conductors improved ENAS and energy recovery. With respect to deionizing salty plasma protein solutions, a MCDI unit featuring highly conductive poly(phenylene alkylene) ionomers and operating under recirculation removed 28% of the salt in the feed concentration while demonstrating 0 to 3% loss of HSA. Overall, MCDI is an effective electrochemical separation platform for deionizing plasma protein solutions.

Acknowledgments

This work was primarily supported through the Membrane Science, Engineering, and Technology (MAST) Center, which is funded by Award # 1841474 from the NSF IUCRC program. This work was also partially supported by the Office of Naval Research (ONR), Award # N00014-22-1-2564. We thank Laura J. Liermann at the LIME Lab at Pennsylvania State University for performing

ICP-OES analysis. We also thank Professor Christian Pester and Sarah Freeburne at Pennsylvania State University for the GPC analysis.

References

(1) de la Rica, R.; Matsui, H. Applications of peptide and protein-based materials in bionanotechnology. *Chemical Society Reviews* **2010**, *39* (9), 3499-3509, DOI: https://doi.org/10.1039/B917574C.
(2) Xu, X.; Hu, J.; Xue, H.; Hu, Y.; Liu, Y.-n.; Lin, G.; Liu, L.; Xu, R.-a. Applications of human and bovine serum albumins in biomedical engineering: A review. *International Journal of Biological Macromolecules* **2023**, *253*, 126914. DOI: https://doi.org/10.1016/j.ijbiomac.2023.126914.
(3) Tao, H.-y.; Wang, R.-q.; Sheng, W.-j.; Zhen, Y.-s. The development of human serum albumin-based drugs and relevant fusion proteins for cancer therapy. *International Journal of Biological Macromolecules* **2021**, *187*, 24-34. DOI: https://doi.org/10.1016/j.ijbiomac.2021.07.080.
(4) Liu, Z.; Chen, X. Simple bioconjugate chemistry serves great clinical advances: albumin as a versatile platform for diagnosis and precision therapy. *Chemical Society Reviews* **2016**, *45* (5), 1432-1456, DOI: https://doi.org/10.1039/C5CS00158G.
(5) Knezevic-Maramica, I.; Kruskall, M. S. Intravenous immune globulins: an update for clinicians. *Transfusion* **2003**, *43* (10), 1460-1480. DOI: https://doi.org/10.1046/j.1537-2995.2003.00519.x.
(6) Saab, W.; Seshadri, S.; Huang, C.; Alsubki, L.; Sung, N.; Kwak-Kim, J. A systemic review of intravenous immunoglobulin G treatment in women with recurrent implantation failures and recurrent pregnancy losses. *American Journal of Reproductive Immunology* **2021**, *85* (4), e13395. DOI: https://doi.org/10.1111/aji.13395 (acccessed 2023/10/30).
(7) Farrugia, A.; Robert, P. Plasma protein therapies: current and future perspectives. *Best Practice & Research Clinical Haematology* **2006**, *19* (1), 243-258. DOI: https://doi.org/10.1016/j.beha.2005.01.002.
(8) Adamski-Medda, D.; Nguyen, Q. T.; Dellacherie, E. Biospecific ultrafiltration: A promising purification technique for proteins? *Journal of Membrane Science* **1981**, *9* (3), 337-342. DOI: https://doi.org/10.1016/S0376-7388(00)80273-2.
(9) Pires, I. S.; Palmer, A. F. Selective protein purification via tangential flow filtration – Exploiting protein-protein complexes to enable size-based separations. *Journal of Membrane Science* **2021**, *618*, 118712. DOI: https://doi.org/10.1016/j.memsci.2020.118712.
(10) Andrew, S. M.; Titus, J. A.; Zumstein, L. Dialysis and Concentration of Protein Solutions. *Current Protocols in Toxicology* **2001**, *10* (1), A.3H.1-A.3H.5. DOI: https://doi.org/10.1002/0471140856.txa03hs10 (acccessed 2023/10/30).
(11) Knudsen, H. L.; Fahrner, R. L.; Xu, Y.; Norling, L. A.; Blank, G. S. Membrane ion-exchange chromatography for process-scale antibody purification. *Journal of Chromatography A* **2001**, *907* (1), 145-154. DOI: https://doi.org/10.1016/S0021-9673(00)01041-4.
(12) Duong-Ly, K. C.; Gabelli, S. B. Chapter Eight - Using Ion Exchange Chromatography to Purify a Recombinantly Expressed Protein. In *Methods in Enzymology*, Lorsch, J. Ed.; Vol. 541; Academic Press, 2014; pp 95-103, DOI: https://doi.org/10.1016/B978-0-12-420119-4.00008-2.
(13) Emin, C.; Kurnia, E.; Katalia, I.; Ulbricht, M. Polyarylsulfone-based blend ultrafiltration membranes with combined size and charge selectivity for protein separation. *Separation and Purification Technology* **2018**, *193*, 127-138. DOI: https://doi.org/10.1016/j.seppur.2017.11.008.

(14) Saxena, A.; Tripathi, B. P.; Kumar, M.; Shahi, V. K. Membrane-based techniques for the separation and purification of proteins: An overview. *Advances in Colloid and Interface Science* **2009**, *145* (1), 1-22. DOI: https://doi.org/10.1016/j.cis.2008.07.004.
(15) Ghosh, R. Separation of human albumin and IgG by a membrane-based integrated bioseparation technique involving simultaneous precipitation, microfiltration and membrane adsorption. *Journal of Membrane Science* **2004**, *237* (1), 109-117. DOI: https://doi.org/10.1016/j.memsci.2004.03.006.
(16) Ghosh, R. Protein separation using membrane chromatography: opportunities and challenges. *Journal of Chromatography A* **2002**, *952* (1), 13-27. DOI: https://doi.org/10.1016/S0021-9673(02)00057-2.
(17) Kreusser, J.; Hasse, H.; Jirasek, F. Adsorption of bovine serum albumin on a mixed-mode resin - influence of salts and the pH value. *Adsorption* **2023**, *29* (3), 163-176. DOI: https://doi.org/10.1007/s10450-023-00384-0.
(18) Niu, C.; Li, X.; Dai, R.; Wang, Z. Artificial intelligence-incorporated membrane fouling prediction for membrane-based processes in the past 20 years: A critical review. *Water Research* **2022**, *216*, 118299. DOI: https://doi.org/10.1016/j.watres.2022.118299.
(19) Alkhadra, M. A.; Su, X.; Suss, M. E.; Tian, H.; Guyes, E. N.; Shocron, A. N.; Conforti, K. M.; de Souza, J. P.; Kim, N.; Tedesco, M.; et al. Electrochemical Methods for Water Purification, Ion Separations, and Energy Conversion. *Chemical Reviews* **2022**, *122* (16), 13547-13635. DOI: https://doi.org/10.1021/acs.chemrev.1c00396.
(20) Gao, F.; Wang, L.; Wang, J.; Zhang, H.; Lin, S. Nutrient recovery from treated wastewater by a hybrid electrochemical sequence integrating bipolar membrane electrodialysis and membrane capacitive deionization. *Environmental Science: Water Research & Technology* **2020**, *6* (2), 383-391, DOI: https://doi.org/10.1039/C9EW00981G.
(21) Kim, N.; Jeon, J.; Chen, R.; Su, X. Electrochemical separation of organic acids and proteins for food and biomanufacturing. *Chemical Engineering Research and Design* **2022**, *178*, 267-288. DOI: https://doi.org/10.1016/j.cherd.2021.12.009.
(22) Arana Juve, J.-M.; Christensen, F. M. S.; Wang, Y.; Wei, Z. Electrodialysis for metal removal and recovery: A review. *Chemical Engineering Journal* **2022**, *435*, 134857. DOI: https://doi.org/10.1016/j.cej.2022.134857.
(23) Kim, Y.-J.; Choi, J.-H. Enhanced desalination efficiency in capacitive deionization with an ion-selective membrane. *Separation and Purification Technology* **2010**, *71* (1), 70-75. DOI: https://doi.org/10.1016/j.seppur.2009.10.026.
(24) Kulkarni, T.; Al Dhamen, A. M. I.; Bhattacharya, D.; Arges, C. G. Bipolar Membrane Capacitive Deionization for pH-Assisted Ionic Separations. *ACS ES&T Engineering* **2023**. DOI: https://doi.org/10.1021/acsestengg.3c00041.
(25) Zhao, Y.; Wang, Y.; Wang, R.; Wu, Y.; Xu, S.; Wang, J. Performance comparison and energy consumption analysis of capacitive deionization and membrane capacitive deionization processes. *Desalination* **2013**, *324*, 127-133. DOI: https://doi.org/10.1016/j.desal.2013.06.009.
(26) Biesheuvel, P. M.; van der Wal, A. Membrane capacitive deionization. *Journal of Membrane Science* **2010**, *346* (2), 256-262. DOI: https://doi.org/10.1016/j.memsci.2009.09.043.
(27) Sun, K.; Tebyetekerwa, M.; Wang, C.; Wang, X.; Zhang, X.; Zhao, X. S. Electrocapacitive Deionization: Mechanisms, Electrodes, and Cell Designs. *Advanced Functional Materials* **2023**, *33* (18), 2213578. DOI: https://doi.org/10.1002/adfm.202213578.

(28) Porada, S.; Zhao, R.; van der Wal, A.; Presser, V.; Biesheuvel, P. M. Review on the science and technology of water desalination by capacitive deionization. *Progress in Materials Science* **2013**, *58* (8), 1388-1442. DOI: https://doi.org/10.1016/j.pmatsci.2013.03.005.
(29) Palakkal, V. M.; Rubio, J. E.; Lin, Y. J.; Arges, C. G. Low-Resistant Ion-Exchange Membranes for Energy Efficient Membrane Capacitive Deionization. *ACS Sustainable Chemistry & Engineering* **2018**, *6* (11), 13778-13786. DOI: https://doi.org/10.1021/acssuschemeng.8b01797.
(30) Palakkal, V. M.; Jordan, M. L.; Bhattacharya, D.; Lin, Y. J.; Arges, C. G. Addressing Spacer Channel Resistances in MCDI Using Porous and Pliable Ionic Conductors. *Journal of The Electrochemical Society* **2021**, *168* (3), 033503. DOI: 10.1149/1945-7111/abedc4.
(31) Lee, W.-H.; Park, E. J.; Han, J.; Shin, D. W.; Kim, Y. S.; Bae, C. Poly(terphenylene) Anion Exchange Membranes: The Effect of Backbone Structure on Morphology and Membrane Property. *ACS Macro Letters* **2017**, *6* (5), 566-570. DOI: https://doi.org/10.1021/acsmacrolett.7b00148.
(32) Pagels, M. K.; Adhikari, S.; Walgama, R. C.; Singh, A.; Han, J.; Shin, D.; Bae, C. One-Pot Synthesis of Proton Exchange Membranes from Anion Exchange Membrane Precursors. *ACS Macro Letters* **2020**, *9* (10), 1489-1493. DOI: https://doi.org/10.1021/acsmacrolett.0c00550.
(33) Galvan, V.; Shrimant, B.; Bae, C.; Prakash, G. K. S. Ionomer Significance in Alkaline Direct Methanol Fuel Cell to Achieve High Power with a Quarternized Poly(terphenylene) Membrane. *ACS Applied Energy Materials* **2021**, *4* (6), 5858-5867. DOI: https://doi.org/10.1021/acsaem.1c00681.
(34) Kitto, D.; Kamcev, J. The need for ion-exchange membranes with high charge densities. *Journal of Membrane Science* **2023**, *677*, 121608. DOI: https://doi.org/10.1016/j.memsci.2023.121608.
(35) Lee, W.-H.; Kim, Y. S.; Bae, C. Robust Hydroxide Ion Conducting Poly(biphenyl alkylene)s for Alkaline Fuel Cell Membranes. *ACS Macro Letters* **2015**, *4* (8), 814-818. DOI: https://doi.org/10.1021/acsmacrolett.5b00375.
(36) Xu, Y.; Jiang, T.; Zhang, X.; Cao, G.; Yang, L.; Wei, H.; Zhou, H. Poly(arylene alkylene)-Based Ion-Exchange Polymers for Enhancing Capacitive Desalination Capacity and Electrode Stability. *Industrial & Engineering Chemistry Research* **2023**, *62* (36), 14601-14610. DOI: https://doi.org/10.1021/acs.iecr.3c02238.
(37) Zhang, J.; Tang, L.; Tang, W.; Zhong, Y.; Luo, K.; Duan, M.; Xing, W.; Liang, J. Removal and recovery of phosphorus from low-strength wastewaters by flow-electrode capacitive deionization. *Separation and Purification Technology* **2020**, *237*, 116322. DOI: https://doi.org/10.1016/j.seppur.2019.116322.
(38) Chrispim, M. C.; Scholz, M.; Nolasco, M. A. Phosphorus recovery from municipal wastewater treatment: Critical review of challenges and opportunities for developing countries. *Journal of Environmental Management* **2019**, *248*, 109268. DOI: https://doi.org/10.1016/j.jenvman.2019.109268.
(39) Ge, Z.; Chen, X.; Huang, X.; Ren, Z. J. Capacitive deionization for nutrient recovery from wastewater with disinfection capability. *Environmental Science: Water Research & Technology* **2018**, *4* (1), 33-39, DOI: https://doi.org/10.1039/C7EW00350A.